Preferential Homing of Tumor-specific and Functional CD8+ Stem Cell-like Memory T Cells to the Bone Marrow

Kang Wu,*†‡ Yongchao Li,§ Shaoying Zhang,*†‡ Nan Zhou,*†‡
Bingfeng Liu,*†‡ Ting Pan,*†‡ Xu Zhang,*†‡ Haihua Luo,*†‡
Zhaofeng Huang,*†‡ Xuefeng Li,§ Hui Zhang,*†‡
and Junsong Zhang*†‡

Summary: The bone marrow (BM) harbors not only hematopoietic stem cells but also conventional memory T and B cells. Studies of BM-resident memory T cells have revealed the complex relationship between BM and immunologic memory. In the present study, we identified CD122high stem cells antigen-1 (Sca-1)high, B-cell lymphoma protein-2 (Bcl-2)high, CD8+ stem cell-like memory T cells (T_{SCM}s) as a distinct memory T-cell subset preferentially residing in the BM, where these cells respond vigorously to blood-borne antigens. We found that the most T_{SCM}s favorably relocate to the BM by adhesion molecules such as vascular cell adhesion protein 1, P-selectin glycoprotein 1, and P-selectin or E-selectin. Moreover, the BM-resident T_{SCM}s exhibited much higher levels of antitumor activity than the spleen-resident T_{SCM}s. These results indicate that the BM provides an appropriate microenvironment for the survival of CD8+ T_{SCM}s, thereby broadening our knowledge of the memory maintenance of antigen-specific CD8+ T lymphocytes. The present findings are expected to be instructive for the development of tumor immunotherapy.

Key Words: CD8+, stem cell-like memory T cells, bone marrow, antitumor immunotherapy

(*J Immunother* 2019;42:197–207)

T memory stem cells (T_{SCM}s), which possess the properties of self-renewal and multipotency, have been observed to play a role in the pathogenesis of various severe diseases such as graft-versus-host disease, malignant melanoma, Chagas disease, as well as human immunodeficiency virus type 1 and simian immunodeficiency virus infections.[1–13] Mouse CD8+ T_{SCM}s are a well-identified subset of postmitotic CD44low CD62Lhigh T cells that express surface proteins, including stem cell antigen-1 (Sca-1), common interleukin (IL)-2, IL-15, receptor β-chain (CD122), as

well as B-cell lymphoma protein-2 (Bcl-2) at high levels. It has been reported that T_{SCM}s could be generated in vitro from naive T cells by activation of the Wnt, IL-7, or IL-15 signaling pathways.[1,2,14] Blood-derived T_{SCM}s have also been tracked in vivo in patients after gene therapy for human severe combined immunodeficiency disease.[15] Similar to conventional memory T cells, CD8+ T_{SCM}s can be detected in umbilical cord blood in humans.[3] Although this phenomenon indicates a tropism for lymphoid tissues, the anatomic characterization of T_{SCM}-cell niches has not been performed to date.

The bone marrow (BM) functions as the major reservoir and site of recruitment for hematopoietic stem cells (HSCs) as well as memory B and T cells by providing appropriate cellular niches.[16–29] The common niche that supports HSCs or leukocytes in the BM is constituted by CXCL12+ stromal cells.[30] Under certain conditions, the BM supports the homeostasis of naive T cells and pro-B cells.[31–33] In addition, BM microvessels constitutively express prerequisite traffic molecules that support the recruitment of HSCs and conventional memory T cells, and potentially support the homing of other T-cell subsets.[34] More importantly, the function of BM-resident CD8+ T cells is distinct from that of those residing in other organs. For instance, BM-resident CD8+ T cells from cancer patients elicit more efficient tumor-specific cytotoxicity than CD8+ T cells in peripheral blood (PB). Thus, T cells from the BM are regarded as potential resources for antitumor cellular therapy.[35] Nevertheless, it is not known whether T_{SCM}s, which constitute a distinct T-cell subset with the highest antitumor activity reported to date, accumulate in the BM.

In the present study, we demonstrate that the BM acts as a hub to which most tumor-specific CD8+ T_{SCM}s relocate. Importantly, BM-resident T_{SCM}s showed higher inhibitory activity against tumor growth than spleen (SP)-resident T_{SCM}s in a B16 murine model, implying potential applications for immunotherapy against melanoma.

RESULTS

CD8+ T Memory Stem Cells Preferentially Reside in the BM

Although T_{SCM}s are categorized as memory cells, they display a naive-like phenotype; these cells include CD62L+ CCR7+ CD45RO− CD45RA+ in humans and CD44low CD62Lhigh in mice.[1–3,36] To determine whether T_{SCM}s reside naturally in the BM, the expression levels of Sca-1 and CD122, which are typical markers used to distinguish T_{SCM}s from naive T cells in mice, were first analyzed in CD44low CD62Lhigh CD8+ T cells (Fig. S1, Supplemental Digital Content 1, http://links.lww.com/JIT/A529). Significant elevation of the CD122high Sca-1high subset was observed in the BM-derived naive T-cell compartment (Fig. 1A, Fig. S2,

Supplemental Digital Content 1, http://links.lww.com/JIT/A529) compared with those from other tissues, including SP, PB, and mesenteric lymph nodes (LN) (Fig. 1B). Thus, we hypothesized that CD122^{high} Sca-1^{high} T$_{SCM}$s preferentially reside in the BM.

Well-defined T$_{SCM}$s express not only high levels of CD122 and Sca-1 but also high levels of Bcl-2 and CXCR3.[1,2] To validate whether these natural CD122^{high} Sca-1^{high} T$_{SCM}$s in the BM are consistent with the previously well-defined T$_{SCM}$s, the expression levels of Bcl-2 and CXCR3 were analyzed in CD122^{high} Sca-1^{high} T$_{SCM}$s and

CD122^{low} Sca-1^{low} naive T cells. As expected, the expression levels of both Bcl-2 and CXCR3 were higher in CD122^{high} Sca-1^{high} T$_{SCM}$s than in naive CD8$^+$ T cells (Figs. 1C, D, Fig. S3, Supplemental Digital Content 1, http://links.lww.com/JIT/A529).[1,2] Similar to BM naive T cells reported previously, BM CD8$^+$ T$_{SCM}$s were also positive for CD127 expression (Fig. 1E).[28] Despite the slightly lower expression of CD127 in BM CD8$^+$ T$_{SCM}$s, the difference was not statistically significant (Fig. S3, Supplemental Digital Content 1, http://links.lww.com/JIT/A529). It is interesting to
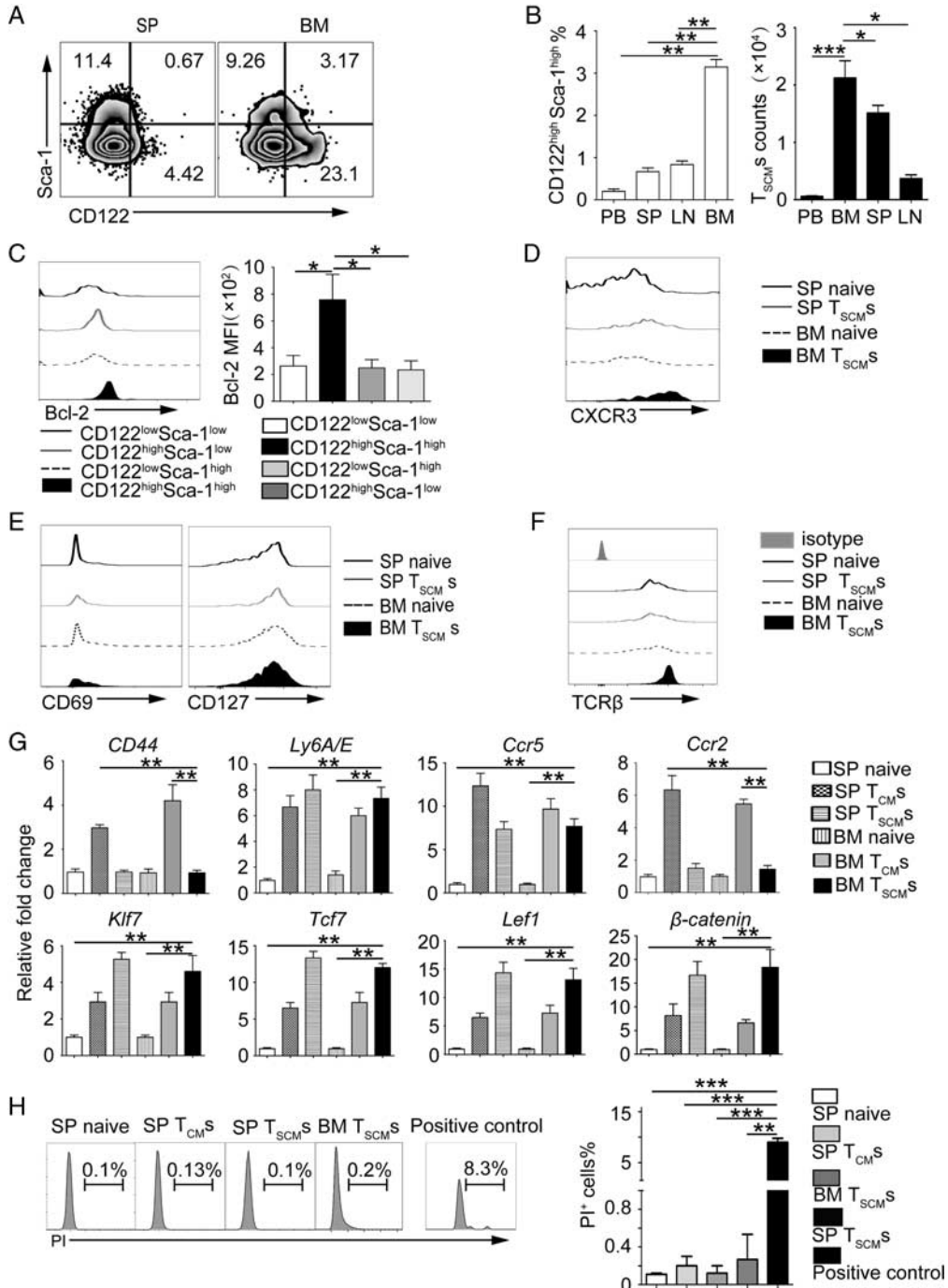
note that, the expression of CD69 in BM-resident T$_{SCM}$s was slightly higher than that of naive T cells (Fig. 1E, Fig. S3, Supplemental Digital Content 1, http://links.lww.com/JIT/A529). Of note, the canonical T$_{SCM}$s reported previously in peripheral immune organs were αβ T cells.[3] Therefore, to eliminate the potential interference of γδ T cells, which also reside in the BM and contain a fraction of cells expressing CD122 and Sca-1 molecules,[37–39] the expression of T-cell receptor (TCR) chains was evaluated by flow cytometry. We found that CD122^{high} Sca-1^{high} T$_{SCM}$s expressed TCRβ chains other than TCRγδ chains (Fig. 1F, Fig. S3, Supplemental Digital Content 1, http://links.lww.com/JIT/A529). In addition, to distinguish between T$_{CM}$s, naive T cells and T$_{SCM}$s in a postmitotic phenotype at the transcriptional level, we tested the expression of *Ccr2, Ccr5, CD44*, and *Sca-1 (Ly6A/E)* by quantitative real-time polymerase chain reaction (qRT-PCR) in accordance with previous reports[1]; results showed that the messenger RNA (mRNA) expression of *Ccr2* in T$_{CM}$s was much higher than in naive T cells and T$_{SCM}$s, whereas the mRNA expression of *Ccr5* in naive T cells was much lower than in T$_{SCM}$s and T$_{CM}$s (Fig. 1G). It is notable that the mRNA expression of *CD44* was lower in T$_{SCM}$s than that in T$_{CM}$s but the mRNA level of *Sca-1 (Ly6A/E)* was significantly higher than that in naive T cells, which was consistent with the previous report (Fig. 1G).[1] According to previous reports, cells with stem cell properties, including HSCs and T$_{CM}$s, are most likely in the resting stage.[20,26,27] In order to verify the stem cell properties of T$_{SCM}$s, we examined the cell cycle of naive T cells, T$_{SCM}$s, and T$_{CM}$s (Fig. 1H, Fig. S4, Supplemental Digital Content 1, http://links.lww.com/JIT/A529). Measurement of DNA content showed that BM CD8$^+$ T$_{SCM}$s were stalled in the G0/G1 cell interphase and resting state; these findings were almost consistent with those for BM memory T cells, as indicated by previous reports (Fig. 1H).[25,40] In addition, we examined other factors (*Klf-7, Tcf-1, Lef-1, β-catenin*) involved in the regulation of stemness of cells by qRT-PCR (Fig. 1G). The qRT-PCR data indicated that the mRNA expression of *Tcf-1, Lef-1*, and *β-catenin* in BM-resident T$_{SCM}$s was notably higher than that in naive T cells (Fig. 1G). Collectively, these observations further support that BM-enriched CD122^{high} Sca-1^{high} naive-like CD8$^+$ T lymphocytes can be identified as T$_{SCM}$s that naturally inhabit the BM.

BM-resident CD8$^+$ T$_{SCM}$s Vigorously Respond to a Blood-borne Antigen

CD8$^+$ T$_{SCM}$s have been shown to elicit rapid immune responses upon antigen rechallenge.[3,41] To investigate the immune responses of CD8$^+$ T$_{SCM}$s in situ, the purified naive T cells (CD8$^+$ CD44^{low} CD62L^{high} CD122^{low} Sca-1^{low}), T$_{CM}$s (CD8$^+$ CD44^{high} CD62L^{high}), and T$_{SCM}$s (CD8$^+$ CD44^{low} CD62L^{high} CD122^{high} Sca-1^{high}) from the BM of OT-I mice (CD45.2$^+$) were adoptively transferred into congenic mice (CD45.1$^+$), respectively, followed by antigen stimulation by ovalbumin (OVA) immunization (Fig. 2A, Fig. S5, Supplemental Digital Content 1, http://links.lww.com/JIT/A529). Flow cytometric analysis showed that the BM T$_{SCM}$s displayed significantly higher levels of cell proliferation and interferon-γ (IFN-γ) production than BM T$_{CM}$s and BM naive T cells (Figs. 2B, C). In addition, to test the downstream differentiation potential of T$_{SCM}$s upon antigen exposure, we compared the frequencies of BM CD44$^+$ T cells in naive T-cell-transferred or T$_{SCM}$s-transferred recipient mice. As expected, we detected larger numbers of CD45.2$^+$ CD44$^+$ CD8$^+$ T cells in T$_{SCM}$s-transferred recipient mice (Fig. 2D), which indicated that the transferred CD8$^+$ T$_{SCM}$s were capable of differentiation into conventional memory or effector T cells more rapidly. These results indicate that BM-enriched CD122^{high} Sca-1^{high} T$_{SCM}$s response to a blood-borne antigen efficiently.

Preferential Migration of CD8$^+$ T$_{SCM}$s to the BM

Owing to the limitation of low cell number of natural CD8$^+$ T$_{SCM}$s from wild-type (WT) mice, it was not practical to obtain the required cell numbers from WT mice on a large scale for investigation of the preferential migration of T$_{SCM}$s to the BM. Although β-catenin signaling was not found to regulate the generation of memory T cells and inhibit T-cell proliferation, T$_{SCM}$s could be generated efficiently from naive T cells in vitro with the glycogen synthase kinase-3β inhibitor TWS119 (a compound that induces T$_{SCM}$ cells by a mechanism of action that is currently debated) as previously reported.[42,43] The naive T cells and in vitro-generated T$_{SCM}$s cells with TWS119 were isolated by flow cytometry (Fig. S6, Supplemental Digital Content 1, http://links.lww.com/JIT/A529). Subsequently, we labeled naive T cells and T$_{SCM}$s with CMTPX and then mixed with

▶ **FIGURE 1.** CD8$^+$ memory stem cells preferentially reside in BM. A, Expression of CD122 and Sca-1 in SP-resident and BM-resident naive-like T-cell compartment. Dot plots represent the frequencies of CD122^{high} Sca-1^{high} subset gated on CD3$^+$CD4$^-$CD8$^+$CD44^{low}CD62L^{high} cells. Data are representative for 6 independent experiments (n = 8). B, T$_{SCM}$s in BM, PB, SP, and LN organs. The frequencies of T$_{SCM}$s accounting for CD44^{low} CD62L^{high} CD8$^+$ T cells and T$_{SCM}$s cell counts in PB, LN, SP, and BM were shown as mean ± SD, 1-way ANOVA. The cell count of CD8$^+$ T$_{SCM}$s was calculated as the formulation: (the total number of cell count)×(CD3$^+$ CD8$^+$)%×(CD44$^-$ CD62L$^+$)%×(CD122$^+$ Sca-1$^+$)%. Data are representative for 4 independent experiments (n = 6). C, Expression of Bcl-2 in naive and T$_{SCM}$ subsets in BM-resident T cells. Overlaid histogram plots show the levels of Bcl-2 in BM-resident CD122^{low} Sca-1^{low}, CD122^{low} Sca-1^{high}, CD122^{high} Sca-1^{low}, and CD122^{high} Sca-1^{high} subsets gated on CD3$^+$CD4$^-$CD8$^+$CD44^{low}CD62L^{high} cells. Data are representative for 5 independent experiments (n = 5). The MFI of Bcl-2 in CD122^{low} Sca-1^{low}, CD122^{low} Sca-1^{high}, CD122^{high} Sca-1^{low}, and CD122^{high} Sca-1^{high} subset was shown as mean ± SD, 1-way ANOVA. D–F, Flow cytometric analysis of SP-resident and BM-resident T$_{SCM}$s overlaid with SP-resident and BM-resident naive T cells. Overlaid histogram plots show expression levels of a given molecule in different CD8$^+$ T-cell subsets. CD8$^+$ T-cell subsets were defined as follows: BM-resident T$_{SCM}$s, CD3$^+$ CD8$^+$CD4$^-$CD44^{low} CD62L^{high}CD122^{high} Sca-1^{high}; BM-resident and SP-resident naive T cells, CD3$^+$ CD8$^+$ CD4$^-$ CD44^{low}CD62L^{high} CD122^{low}Sca-1^{low}. Data are representative for 5 independent experiments (n = 7). G, RT-PCR results show the expressions of *Klf-7, Tcf-1, Lef-1, β-catenin, Ccr2, Ccr5, CD44*, and *Sca-1* in different CD8$^+$ T-cell subsets. CD8$^+$ T-cell subsets were defined as follows: BM-resident T$_{SCM}$s, CD3$^+$ CD8$^+$ CD4$^-$ CD44^{low} CD62L^{high} CD122^{high} Sca-1^{high}; BM-resident and SP-resident naive T cells, CD3$^+$ CD8$^+$ CD4$^-$ CD44^{low}CD62L^{high} CD122^{low} Sca-1^{low}; BM-resident and SP-resident T$_{CM}$s, CD3$^+$ CD8$^+$ CD4$^-$ CD44^{high} CD62L^{high}. Data were shown as mean ± SD, 1-way ANOVA. H, CD8$^+$ naive T cells and T$_{SCM}$s from BM, SP, of C57BL/6 mice and their DNA stained with PI. For the positive control of PI staining, the 2×10^6 SP cells from C57BL/6 mice were stimulated with anti-CD3 (2 μg/mL) and anti-CD28 (1 μg/mL) in the presence of IL-2 (10 ng/mL). Histograms show the percentage of DNA content in different CD8$^+$ T-cell subsets. Data are representative for 3 independent experiments (n = 5). Data were shown as mean ± SD, 1-way ANOVA (*P < 0.05, **P < 0.01, ***P < 0.001). ANOVA indicates analysis of variance; BM, bone marrow; LN, lymph nodes; PB, peripheral blood; PI, propidium iodide; SP, spleen.
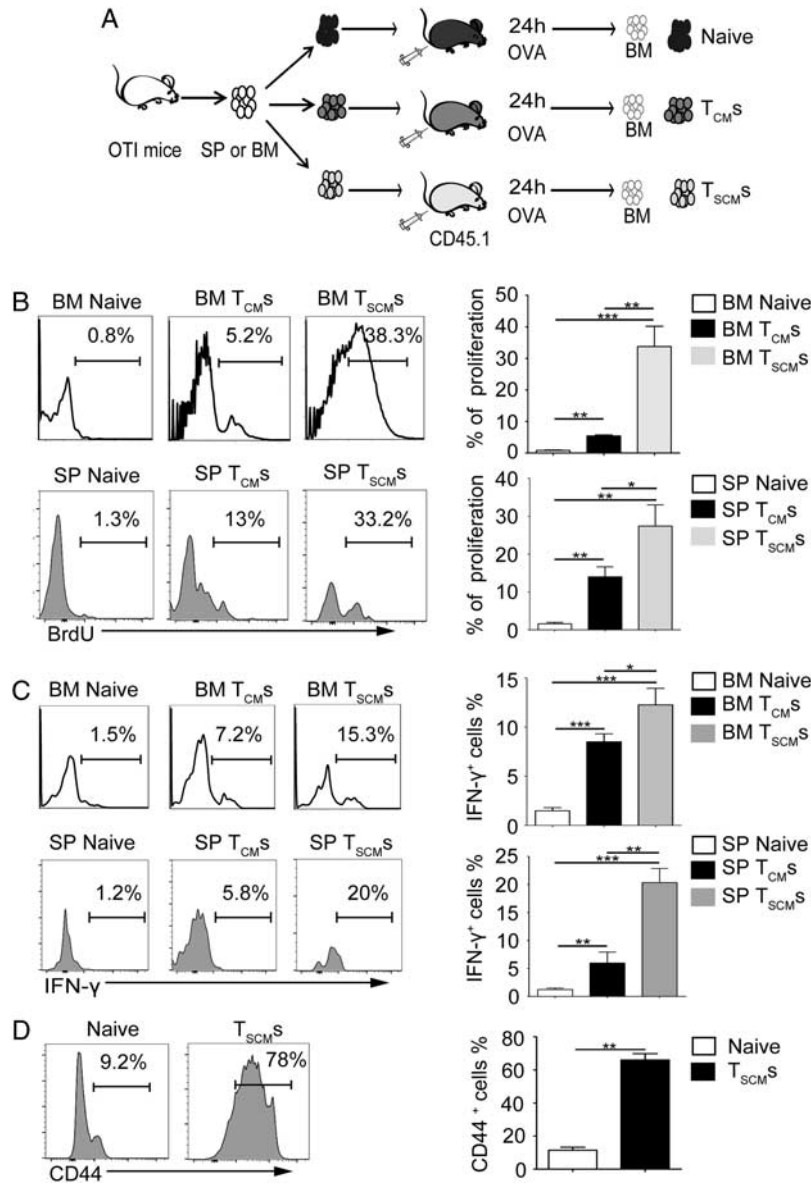
FIGURE 2. CD8^{+} TSCMs from BM can respond to blood-borne antigen in vivo. A, Schematic diagram of adoptive transfer. B and C, BM-resident T_{SCM}s possess the capacity of rapidly acquiring effector functions in vivo. The 5×10^5 each subset of T cells from BM of OT-Imice were adoptively transferred to CD45.1 mice, respectively. Recipients were immunized with 500 μg OVA in CFA and sacrificed after 3 days for further analysis. The T-cell subsets were determined by the following FACS isolations: CD45.2^{+} CD8^{+} CD44^{low} CD62L^{high} CD122^{low} Sca-1^{low} for naive T cells; CD45.2^{+} CD8^{+} CD44^{low} CD62L^{high} CD122^{high} Sca-1^{high} for T_{SCM}s; CD45.2^{+} CD8^{+} CD44^{high} CD62L^{high} for T_{CM}s. B, Numbers in histograms represent the percentage of BrdU-positive cells in BM-resident naive, T_{CM} and T_{SCM} cells after OVA stimulation. C, Intracellular cytokine staining of naive, T_{CM} and T_{SCM} cells in BM. Numbers in histograms show the percentage of IFN-γ-expressing cells in BM after OVA stimulation. Data are representative for 3 independent experiments (n = 6). Frequencies of BrdU^{+} (B) and IFN-γ^{+} cells (C) were shown as mean ± SD, *t* test. D, In vitro-generated CD8^{+} T_{SCM}s possess the capacity of rapidly acquiring effector functions in vivo. The 1×10^6 purified in vitro-generated CD8^{+} T_{SCM}s with TWS119 or 1×10^6 purified natural naive T cells were adoptively transferred into CD45.1 mice and then were immunized with 500 μg OVA in CFA per mice by injection intraperitoneally. Three days after immunization, the expressions of CD44 molecule were detected. Histograms show the percentage of the CD44^{+} CD45.2^{+}CD8^{+} T cells (n = 3). Data were shown as mean ± SD, 1-way analysis of variance (*P < 0.05, **P < 0.01, ***P < 0.001). BM indicates bone marrow; CFA, complete Freund's adjuvant; IFN-γ, interferon-γ; OVA, ovalbumin.

equivalent carboxyfluorescein succinimidyl ester (CFSE)-labeling SP cells, which served as a reference. The mixed cells were injected into recipient mice. After 6 hours, we detected the ratios of CMTPX-positive and CFSE-positive cells, and calculated the homing index (HI). The results showed that the HI of TWS119-induced T_{SCM}s in the BM was ~3-fold higher than that of those induced in the SP (Fig. 3A). To accurately compare the homing of each subset and avoid the off-target effects of small-molecule inhibitors, T_{SCM}s were generated by stimulation of Wnt3A protein in vitro, and the frequency of each subset in the BM was determined. Flow cytometric analysis showed that the proportion
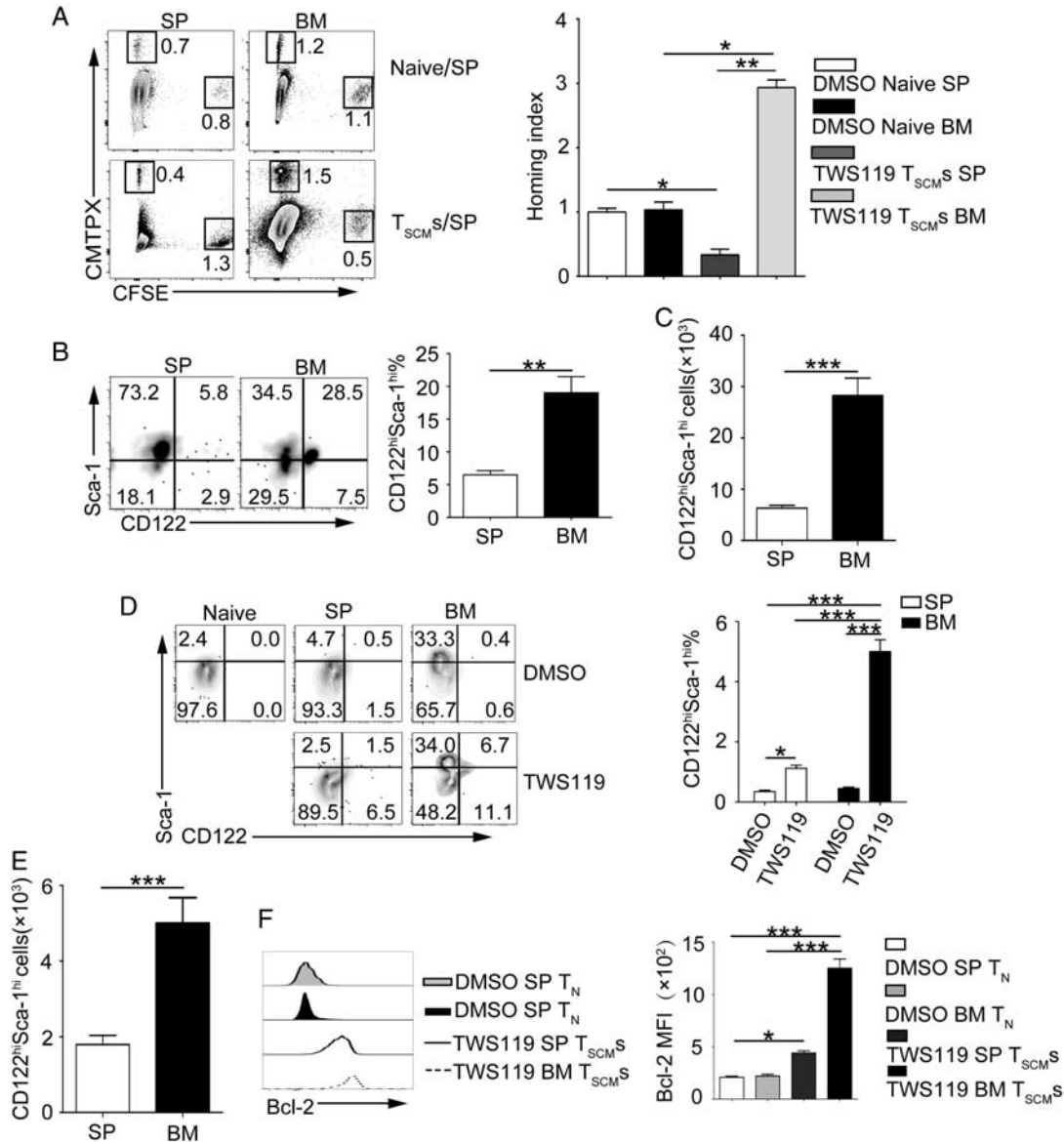
Copyright © 2019 The Author(s). Published by Wolters Kluwer Health, Inc.

FIGURE 3. Homing of $T_{SCM}s$ to BM. A–C, Homing of in vitro-generated CD8$^+$ $T_{SCM}s$. A, Comparison of the homing index of naive T cells and CD8$^+$ $T_{SCM}s$. The 1×10^6 purified naive T cells (top panel) or in vitro-generated CD8$^+$ $T_{SCM}s$ (bottom panel) were labeled with CMTPX (10 μM) and then mixed with CFSE-labeled (10 μM) total SP cells (as a reference) at ratio of 1:1, respectively. The mixed cells were injected into recipient mice. After 6 hours, the ratios of CMTPX-positive cells and CFSE-positive cells were tested by flow cytometry. The numbers in dot plots show the frequencies of CMTPX-positive cells and CFSE-positive cells. Data are representative for 4 independent experiments (n = 6). Homing index was represented as mean ± SD, t test. B, Frequencies of transferred $T_{SCM}s$ in SP and BM. 1×10^6 Wnt3A-treated CD44^{low} CD62L^{high} T cells were injected intravenously and analyzed for transferred $T_{SCM}s$ after 24 hours. Dot plots represent the expression of CD122 and Sca-1 on the surface of CD44^{low}CD62L^{high} adoptive T cells. T-cell subsets were defined as in Figure 2A and Figure S4. Data are representative for 4 independent experiments (n = 6). Frequencies of CD122^{high} Sca-1^{high} subset were shown as mean ± SD, t test. C, Numbers of transferred $T_{SCM}s$ in SP and BM. Data were representative for 4 independent experiments (n = 6). The numbers of CD45.2$^+$ CD8$^+$ CD44^{low} CD62L^{high} CD122^{high} Sca-1^{high} cells were shown as mean ± SD, t test. D–F, In vivo-generated CD8$^+$ $T_{SCM}s$ preferentially homed to the BM. The 2×10^6 splenic CD44^{low} CD62L^{high}CD8$^+$ T cells sorted from OT-I mice were adoptively transferred to CD45.1 mice. The recipients were injected intraperitoneally. 500 μg ovalbumin with complete Freund's adjuvant and 4 doses per day of TWS119 (20 mg/kg) or DMSO (as control) from day 0 to day 3. Mice were sacrificed and analyzed for the expressions of CD122, Sca-1, and Bcl-2 of CD44^{low} CD62L^{high} transferred CD8$^+$ T cells in SP and BM after 1 week. T-cell subsets were determined as Figure 2C and D. D, Dot plots represent the expression levels of CD122 and Sca-1 on the surface of CD44^{low} CD62L^{high} transferred T cells. E, Number of CD8$^+$ $T_{SCM}s$ relocated to SP and BM in vivo. F, Overlaid histograms represent the levels of Bcl-2 in CD44^{low} CD62L^{high} transferred CD8$^+$ T cells with treatment of TWS119 and freshly isolated naive T cells from SP (T_N). Data are representative for 4 independent experiments (n = 6). Frequencies of CD122^{high} Sca-1^{high} subset were shown as mean ± SD, 1-way ANOVA (D). Numbers of CD45.2$^+$ CD8$^+$ CD44^{low} CD62L^{high} CD122^{high} Sca-1^{high} cells were shown as mean ± SD, 1-way ANOVA (E). MFI of Bcl-2 was shown as mean ± SD, 1-way ANOVA (F) (*$P < 0.05$, **$P < 0.01$, ***$P < 0.001$). ANOVA indicates analysis of variance; BM, bone marrow; CFA, complete Freund's adjuvant; CFSE, carboxyfluorescein succinimidyl ester; DMSO, dimethyl sulfoxide; IFN-γ, interferon-γ; OVA, ovalbumin; SP, spleen.

of the CD122^{high} Sca-1^{high} subpopulation in the BM increased by ~5-fold compared with that in the SP (Fig. 3B). Consistently, the number of T_{SCM}s grew significantly when compared with that in the SP (Fig. 3C). As previously reported, CD8$^+$ T_{SCM}s could be generated by activating CD8$^+$ T cells in vivo, when coupled with pharmacological activation of Wnt signaling.[2] To mimic physiological conditions, a relatively low dose of TWS119 was injected intraperitoneally into mice whose T cells were activated by OVA injection to facilitate the minimum generation of T_{SCM}s in vivo (Fig. S7, Supplemental Digital Content 1, http://links.lww.com/JIT/A529).[2] The ratios and numbers of CD122^{high}Sca-1^{high} T_{SCM}s significantly increased in both BM and SP upon TWS119 treatment (Fig. 3D). In particular, the number and ratio of T_{SCM}s in the BM was 4- to 5-fold higher than that in the SP (Figs. 3D, E, Fig. S2, Supplemental Digital Content 1, http://links.lww.com/JIT/A529). In addition, the expression of Bcl-2 was upregulated in BM-resident T_{SCM}s compared with that in their SP-derived counterparts or freshly isolated SP-derived naive T cells (Fig. 3F). Taken together, these results demonstrate that the CD122^{high} Sca-1^{high} T_{SCM}s preferentially homed to the BM.

P-Selectin or E-Selectin/P-Selectin Glycoprotein 1 (PSGL-1) and Vascular Cell Adhesion Protein 1 (VCAM-1) Mediate the Homing of T_{SCM}s to the BM

The translocation of CD8$^+$ T_{CM}s and HSCs to BM microvessels is dependent on the interactions between adhesion molecules such as VLA-4/VCAM-1 (CD106), P-selectin and E-selectin/PSGL-1, or CXCL-12/CXCR4.[18,25,44,45] Given the similar homing properties of T_{SCM}s, T_{CM}s, and HSCs, studies of the homing of T_{CM} and HSCs may help to elucidate the mechanism underlying the homing of T_{SCM}s. To verify this hypothesis, the expression of candidate adhesion molecules in BM and SP was determined by flow cytometry. The results showed that adhesion molecules, including LFA-1, CXCR4, integrin α4β7, and PSGL-1, were involved in T-cell homing and did not exhibit significant differences in expression (Fig. 4A, Fig. S8, Supplemental Digital Content 1, http://links.lww.com/JIT/A529).[18,46,47] Of note, integrin-α2, a key mediator of the homing of CD4$^+$ memory T cells to the BM, was detected at a low level on the surface of T_{SCM}s (Fig. 4A, Fig. S8, Supplemental Digital Content 1, http://links.lww.com/JIT/A529).[20] P-selectin and E-selectin as well as VCAM-1 molecules are detected in the normal BM sinusoid. It is interesting to note that, the expression of VCAM-1 was moderately higher in BM-resident T_{SCM}s than in naive T cells (Fig. 4A, Fig. S8, Supplemental Digital Content 1, http://links.lww.com/JIT/A529). To determine whether these adhesion molecules mediate the homing of T_{SCM}s to the BM, we generated T_{SCM}s cells with TWS119 in vitro and isolated T_{SCM}s by flow cytometry. CD8$^+$ T_{SCM}s were labeled with CMTPX and then mixed with CFSE-labeling SP cells at ratio of 1:1. The mixed cells were injected into recipient mice, followed by the injection of corresponding antibodies intravenously 6 hours later. After 1 day, we examined the ratios of CMTPX-positive and CFSE-positive cells and calculated the HI. Compared with treatment with immunoglobulin G, flow cytometric analysis showed that the treatment with anti-VCAM-1, anti-P-selectin, anti-E-selectin, or anti-PSGL-1 antibodies significantly downregulated the homing of T_{SCM}s into the BM (Figs. 4B, C). In addition, treatment with anti-CXCL-12 did not result in significant differences in the homing of T_{SCM}s into all the organs (Figs. 4B, C). Together, these data indicate that P-selectin, E-selectin, PSGL-1, and VCAM-1 are the key mediators of the homing of T_{SCM}s.

BM-resident T_{SCM}s Have Enhanced Antitumor Activity Relative to SP-resident T_{SCM}s in Response to Tumor-Antigen Challenge

Tumor-specific cytotoxic T cells or chimeric antigen receptor T cells are currently applied clinically for targeted cancer therapy. The B16 murine melanoma model is useful for the study of malignant melanoma in humans.[31] In order to perform OVA-specific OT-I mice for studying T_{SCM} specificity against tumor antigens, we constructed the B16-OVA cell line as previously described. We hypothesized that the microenvironment of the BM enables the generation of T_{SCM}s with higher antitumor activity; accordingly, we generated OVA-specific CD8$^+$ T_{SCM}s in vivo via injection of TWS119 and tested the antitumor activities. As expected, the BM-derived T_{SCM}s possessed higher antitumor reactivity than the SP-derived T_{SCM}s in the adoptive transfer experiment (Fig. 5A). Furthermore, the transfer of BM-derived T_{SCM}s significantly extended the survival of mice compared with that achieved following the transfer of SP-derived T_{SCM}s (Fig. 5B). Thus, the results suggest that the adoptively transferred BM-derived T_{SCM}s exhibited enhanced antitumor activity and higher therapeutic efficacy than conventional SP-derived T_{SCM}s in mice.

DISCUSSION

In this study, CD8$^+$ T_{SCM}s that highly expressed CD122, Sca-1, Bcl-2, and CXCR3 were identified within the BM-resident naive-like T-cell compartments. Although a small number of natural T_{SCM}s were detected in the peripheral lymphoid organs, including in the SP, PB, or LN, the ratios of natural T_{SCM}s in these organs were much lower than those in the BM. Notably, similar to SP-derived T_{SCM}s, the BM-resident T_{SCM}s were capable of acquiring effector functions more rapidly upon blood-borne antigen exposure than naive T cells. These data also suggest that T_{SCM}s significantly accumulated in the BM, rather than being simply confined to peripheral inflammatory sites. Nevertheless, the differences in species (mouse and nonhuman primates) resulted in differences in the distribution of CD8$^+$ T-cell subsets in lymphoid organs, which was manifested in the distribution of CD8$^+$ T_{CM}s (larger numbers of mouse CD8$^+$ T_{CM}s in BM, in contrast with larger numbers of rhesus CD8$^+$ T_{CM}s in the LNs).[9] Further, the distribution of CD8$^+$ T_{SCM}s in mice was different from that in nonhuman primates. Therefore, the natural distribution of CD8$^+$ T_{SCM}s in the human body requires further in-depth study. In addition, our data provided novel insights into the cytotoxic activity of T_{SCM}s in the BM, whose function has thus far been ambiguous, and suggested a possible mechanism for the enhanced antitumor activity of BM T cells.

Despite the concomitant expression of numerous markers of naive T cells on the surface of T_{SCM}s, both bioinformatics analysis of microarray data and antigenic stimulation experiments have suggested that T_{SCM}s are most closely related to T_{CM}s.[3] However, it remains unknown whether the other characteristics of T_{SCM}s, especially the trafficking properties, are similar to those of T_{CM}s. The BM plays an important role in controlling immune responses by influencing the generation of lymphocytes and the maintenance of immunologic memory.[16] Through investigations of the homing and retention of T_{SCM}s in the BM, we found that both in vivo-generated and in vitro-generated T_{SCM}s preferentially relocated to the BM (Fig. 3). Unfortunately, the results of the homing assay with CD8$^+$ T_{SCM}s generated by Wnt3A protein in vitro were not absolutely consistent with the results of in vivo studies. We speculated that introduction in vitro may be more efficient. Therefore, the
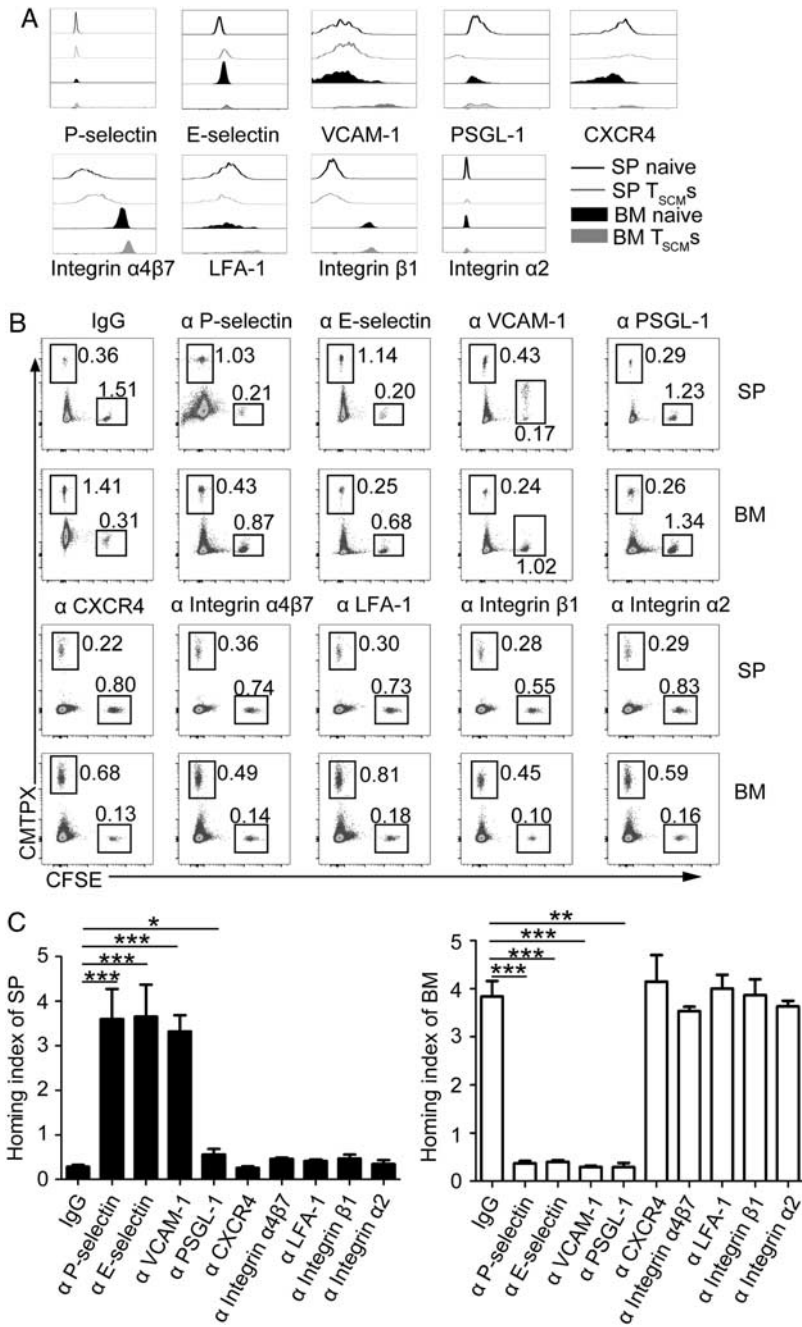
FIGURE 4. Adhesion molecules for T$_{SCM}$s homing to the BM. A, Expression levels of adhesion molecules on the surface of T$_{SCM}$s. Overlaid histogram plots show expression levels of a given molecule in different CD8$^+$ T-cell subsets. CD8$^+$ T-cell subsets were defined as Figure 1D–F. Data are representative for 3 independent experiments (n = 6). B, Effect of monoclonal antibodies on T$_{SCM}$s homing to BM vessels. The CMTPX-labeled (10 μM) 1×10^6 purified in vitro-generated CD8$^+$ T$_{SCM}$s with TWS119 and then mixed with CFSE-labeled (10 μM) total SP cells (as a reference) at ratio of 1:1. The mixed cells were injected into recipient mice. After 6 hours, the mice were injected with 100 μg of neutralizing antibodies and IgG control intravenously per mice and analyzed for homing index in SP and BM after 24 hours. C, Data are representative for 3 independent experiments (n = 4). Data were shown as mean ± SD, 1-way analysis of variance (*P < 0.05, **P < 0.01, ***P < 0.001). BM indicates bone marrow; CFSE, carboxyfluorescein succinimidyl ester; IgG, immunoglobulin G; PSGL-1, P-selectin glycoprotein 1; SP, spleen; VCAM-1, vascular cell adhesion protein 1.

homing efficacy of in vivo-generated T$_{SCM}$s was higher than that of in vitro-generated T$_{SCM}$s. Although T$_{SCM}$s could be induced from naive T cells in vivo and were detected in the BM, the anatomic sites of transition from the naive state have not yet been determined.

The process of the accumulation of leukocytes in tissue depends on a series of adhesive interactions with vessels that involve tethering, rolling, or sticking. Although each adhesion procedure is mediated by several specific receptor-ligand pairs, each leukocyte possesses its own indispensable,
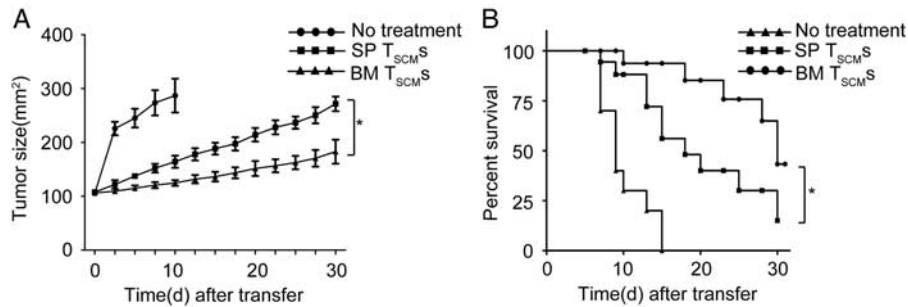
FIGURE 5. Antitumor activity in vivo of BM-resident T_{SCM}s. B16-OVA cells (1.5×10^6 per mice) were injected intradermally to establish tumor mice model in WT mice. After 10 days, the 5×10^4 in vivo-generated OVA-specific T_{SCM}s, which were isolated from SP or BM of CD45.1 recipient mice after the stimulation of OVA in the presence of TWS119 for 7 days, were adoptively transferred into the tumor-bearing mice. Tumor size (mm^2) (A) and survival (percent survival) (B) of WT mice were measured. Data are represented as mean $\pm$ SD, log rank, *$P < 0.05$. All data shown are representative of at least 2 independent experiments (n = 5). BM indicates bone marrow; OVA, ovalbumin; SP, spleen; WT, wild type.

subset-specific set of traffic molecules. We have demonstrated that the homing of T_{SCM}s to the BM is dependent on adhesive interactions between T_{SCM}s and BM vessels. Furthermore, the blocking experiment with certain antibodies resulted in a dramatic decline of BM-resident T_{SCM}s in vivo, whereas the CD8$^+$ T_{SCM} were arrested in the SP. CD8$^+$ T_{SCM}s, as a long-term subset, would be relocated to the immune organs in favor of their own self-renewal. SP, as the largest peripheral lymphoid organ, is one of the main locations at which the CD8$^+$ T_{SCM}s are arrested. Therefore, the migration of CD8$^+$ T_{SCM}s to the SP is indispensable when their migration to the BM is blocked. This phenomenon suggests that all 4 adhesion molecules analyzed in our study, namely P-selectin, E-selectin, PSGL-1, and VCAM-1, act as mediators for the homing of T_{SCM}s into the BM. A significant decline of T_{SCM}s in the SP was observed after injection of anti-PSGL-1. Of note, P-selectin and E-selectin as well as VCAM-1 are enriched in BM microvessels, whereas PSGL-1, the ligand of P-selectin and E-selectin, is expressed on most immune cells and facilitates the homing of resting T cells into lymphoid organs.[48] Therefore, the mechanism underlying the presence of T_{SCM}s in the BM involves adhesive interactions between PSGL-1 and P-selectin or E-selectin, whereas T_{SCM}s appear to home to the SP in a PSGL-1-independent manner. In particular, VCAM-1, the adhesion protein expressed in T_{SCM}s and microvessels, was found to be crucial for the homing of T_{SCM}s into the BM rather than into the SP; however, we have not yet identified the specific tissue-resident molecules that predominate in this process. The administration of various neutralizing antibodies altered the BM microenvironment surrounding the BM-resident CD8$^+$ T_{SCM}s and blocked the homing of CD8$^+$ T_{SCM}s into the BM. Under such conditions, the adoptively transferred CD8$^+$ T_{SCM}s were retained in the PB. Our data elucidate the specific migratory routes of T_{SCM}s to the BM. Nevertheless, there may be additional unidentified factors involved in this process. The induction of adhesion-related molecules appears to be a critical step in the development of a stable T_{SCM} compartment in the BM; however, the underlying mechanism merits further investigation. In contrast to previous reports describing the relocation of CD8$^+$ T_{CM}s in BM, the homing of CD8$^+$ T_{SCM}s did not seem to be dependent on CXCL-12.[18] In a previous study, the dependence of memory T-cell homing to the BM on CXCL12 was strongly implicated, with reduced integrin activation after anti-CXCL12 treatment.[18] We attempted to confirm the changes of integrin activation in CD8$^+$ T_{SCM}s; however, no differences were observed, at least in integrin-$\alpha 4 \beta 7$,

integrin-$\alpha 2$, and integrin-$\beta 1$ protein. It was speculated that the CD8$^+$ T_{SCM} subset is different from CD8$^+$ T_{CM} subset at this point, as they are 2 different subsets.

An appropriate microenvironment for BM-resident T_{SCM}s requires conditions that facilitate the homeostasis of T_{SCM}s in specific areas. In particular, the microenvironment in the BM provides not only a homeostatic proliferation signal but also a survival signal by upregulating the expression of Bcl-2 for the maintenance of T_{SCM}s. The cellular DNA content, which was determined by detection using propidium iodide (PI), indicated that BM-resident T_{SCM}s were in a resting status and represented a certain degree of stem cell characteristics; however, the expression of CD69 in BM-resident T_{SCM}s was slightly higher than that in naive T cells. Simultaneously, BM-resident T_{SCM}s could be reactivated rapidly upon exogenous antigen invasion, which suggests that active T_{SCM}s are more likely to reside in areas close to APCs. We speculate that antigen-specific responses may be accompanied by the confluence of T_{SCM}s into large aggregates with several APCs, leading to the activation of T_{SCM}s in the BM. Given that a minority of T_{SCM}s was found in the peripheral immune organs and a large number of T_{SCM}s accumulated in inflammatory sites rapidly, we proposed that these cells utilized the niches in the BM as a refuge, and could be temporarily hidden from antigenic exposure before executing immunologic surveillance.

Our data indicate that the BM-resident T_{SCM}s exert much stronger antitumor activity, which may be instructive for development of tumor immunotherapy. In melanoma patients, high frequencies of tumor-specific T cells were detected. However, most of these cells were anergic or nonresponsive.[49,50] Compared with other subsets, T_{SCM}s show higher antitumor activity. Although the expression of IFN-γ and cell proliferation of natural SP-derived T_{SCM}s was almost equal to those of natural BM-derived T_{SCM}s, we exploited the fact that the microenvironment in the BM could generate more functional and tumor-specific T_{SCM}s in vivo. In addition, we demonstrated that the in vivo-generated T_{SCM}s derived from the BM could significantly extend the survival of mice compared with SP-derived T_{SCM}s. Therefore, the present work showed that the BM microenvironment was more conductive to the induction of functional CD8$^+$ T_{SCM}s; however, the underlying mechanisms remain unknown and need further study. Of note, in the present work, approximately half of the mice with BM T_{SCM}s died, although the tumors were still small. We speculate that tumor metastasis occurs in the B16 model,

despite subcutaneous injection as previously described.[51] Therefore, tumor migration may lead to the death of mice in the B16 model, even when the tumor size is not very large.[2] Our data suggest that the selection of an appropriate microenvironment for tumor-specific T_{SCM}s represents a novel strategy to improve the efficacy of anti-tumor immunotherapies.

Overall, our study has demonstrated that T_{SCM}s, a distinct memory cell subset, exist naturally in WT mice and principally accumulate in the BM. In addition, the present findings show that PSGL-1 interacted with P-selectin and E-selectin to mediate the homing of T_{SCM}s to the BM. In addition, VCAM-1 appears to be involved in this process. Moreover, these findings should contribute to the development of effective antitumor immunotherapy strategies by potentially enabling the production of tumor-antigen–specific T_{SCM}s for patients with cancer.

MATERIALS AND METHODS

Mice

OT-I, C57BL/6J, and CD45.1 (B6.SJL-Ptprc^a^Pep3^b^/BoyJ) mice were purchased from Jackson Laboratories and bred under specific pathogen-free conditions at Sun Yat-Sen University. All experiments performed on mice were approved by the Institutional Animal Care and Use Committee of Sun Yat-Sen University.

Flow Cytometry and Sorting

Single-cell suspensions were prepared from SP, mesenteric LN, blood, or BM of individual mice. For cell staining, cells were preincubated in 0.1% bovine serum albumin/phosphate-buffered saline solution of 10 μg/mL anti-FcgRII/III (2.4G2) (BD Pharmingen, San Jose, CA) for 10 minutes at 4°C. The cells were then stained for 20 minutes at 4°C with primary antibodies. For cell sorting, BD FACS AriaII cell sorter (BD Biosciences, San Jose, CA) was used. For intracellular cytokine staining, cells were stimulated with phorbol 12-myristate 13-acetate (100 ng/mL; Sigma-Aldrich, St. Louis, MO) and ionomycin (1 μg/mL; Sigma-Aldrich) in the presence of 5 μg/mL brefeldin A (Sigma-Aldrich) for 4 hours. Cells were washed twice in phosphate-buffered saline, and then fixed and permeabilized with BD Cytofix/Cytoperm Fixation/Permeabilization Kit. Stained samples were analyzed in BD LSR II Fortessa (BD Biosciences). Flow cytometric data were analyzed with FlowJo (Tree Star) software.

Primary antibodies used in the study include anti-CD62L (MEL-14) (eBiosciences, San Diego, CA), anti-CD45.2 (104) (eBiosciences), anti-CD44 (IM7) (eBiosciences), anti-CD3 (145-2C11) (eBiosciences), anti-Sca-1 (D7) (BD Pharmingen), anti-CD8 (53-6.7) (eBiosciences), anti-TCRβ (H57-597) (eBiosciences), anti-LFA-1 (H155-78) (eBiosciences), anti-IFN-γ (XMG1.2) (eBiosciences), anti-CD4 (RM4-5) (eBiosciences), anti-5-bromo-2'-deoxyuridine (BrdU) (3D4) (eBiosciences), anti-CD69 (H1.2F3) (eBiosciences), anti-CD127 (A7R34) (eBiosciences), anti-CXCR4 (2B11) (eBiosciences), anti-VCAM-1 (429) (eBiosciences), anti-CD62P (RB40.34) (BD Pharmingen), anti-CD29 (eBioHMb1-1) (BD Pharmingen), anti-CD183 (CXCR3-173) (BD Pharmingen), anti-Bcl-2 (3F11) (BD Pharmingen), anti-integrin-α4β7 (DATK32), anti-CD162 (2PH1) (eBiosciences), and anti-CD62E (P2H3) (eBiosciences).

qRT-PCR

Total RNA was isolated with TRIzol reagent (Life Technologies) and then subjected to complementary DNA (cDNA) synthesis with PrimeScript reverse transcription (RT) reagent kit (TaKaRa, Shiga, Japan). All primers were annealed at 37°C and RT was performed at 42°C. Quantitative PCR was performed with SYBR premix Ex Taq II kit (TaKaRa) following the manufacturer's instructions. Sequences of primers are listed in Supplemental Table I (Supplemental Digital Content 1, http://links.lww.com/JIT/A529).

Generation of TSCM Cells In Vivo and In Vitro

The CD44^low^CD62L^high^ cells were stimulated with 2 μg/mL anti-CD3 (BD Pharmingen), 1 μg/mL anti-CD28 (BD Pharmingen), and 10 ng/mL IL-2 (Peprotech, Rocky Hill, NJ) in the presence of TWS119 (7 μM) (Selleckchem, Houston, TX) or Wnt3A protein (1 μg/mL) (Peprotech) in vitro. For generation of T_{SCM}s in vivo, $2×10^6$ OT-I naive CD8^+^ T cells were adoptively transferred into congenic CD45.1 mice and then injected intraperitoneally (500 μg) per mouse OVA (Sigma-Aldrich) with complete Freund's adjuvant (CFA) (Sigma). Mice received 4 doses per day of TWS119 at 40 mg/kg from day 0 to day 3. Six days after injection, mice with or without the treatment of TWS119 were sacrificed for further analysis. The CD8^+^ T_{SCM}s were isolated by flow cytometry on the basis of the expression of surface markers (CD3^+^ CD4^−^ CD8^+^ CD62L^+^ CD44^−^ CD122^+^ Sca-1^+^ T cells for in vitro-generated T_{SCM}s or CD45.1^+^ CD8^+^ CD62L^+^ CD44^−^CD122^+^ Sca-1^+^ T cells for in vivo-generated T_{SCM}s).

In Vivo Activation of CD8^+^ T Cells

Cells of 3 T-cell subsets [$5×10^5$; naive T cells: CD3^+^ CD8^+^ CD62L^+^ CD44^−^ Sca-1^−^ CD122^−^; central memory T cells (T_{CM}s): CD3^+^ CD8^+^ CD62L^+^ CD44^+^; T_{SCM}s: CD3^+^ CD8^+^ CD62L^+^ CD44^−^ Sca-1^+^ CD122^+^] from SP or BM of OT-I mice were adoptively transferred to CD45.1 mice. Recipients were immunized with 500 μg of OVA in CFA and sacrificed after 3 days for further analysis.

Cell Proliferation

Cell proliferation in vitro was determined by BrdU staining. CD44^low^ CD62L^high^ T cells (at a concentration of $2×10^6$/mL from SP or BM were cultured in RPMI 1640 medium (Gibco, Carlsbad, CA) containing 9% fetal bovine serum (Gibco, Carlsbad, CA), penicillin (100 U/mL) (Hyclone; GE Healthcare Life Sciences, Chicago, IL), and streptomycin (100 μg/mL) (Hyclone; GE Healthcare Life Sciences). For the activation of C57BL/6J mice-derived T cells, cells were stimulated with anti-CD3 (2 μg/mL) and anti-CD28 (1 μg/mL) (BD Pharmingen) in the presence of IL-2 (10 ng/mL) (Peprotech). For the activation of OT-I mice-derived T cells, experiments were performed in accordance with previously described protocols.[52] Briefly, $1×10^6$/mL T cells were cocultured with $2×10^7$/mL irradiated T-depleted SP or BM-derived antigen-presenting cells in the presence of OVA~257–264~ peptides (*SIINFEKL*) (2 μM) (Anaspec, San Jose, CA) and IL-2 (10 ng/mL) (Peprotech).

BrdU Labeling

For in vitro labeling with BrdU, cells were stimulated and then incubated with BrdU at a final concentration of 10 μM in cell culture medium before being harvested at 16 hours. For the in vivo proliferation assay, BrdU was diluted at a concentration of 10 mg/mL as a stock solution; then, 200 μL of the stock solution was injected into each mouse.

Homing Assay

Homing experiments of CMTPX-labeled TWS119-induced or vehicle-treated control cells and CFSE-labeled reference cells were performed as described previously, with

some modifications.[53] Briefly, 2×10^6 CMTPX-labeled (10 μM) TWS119-induced CD8$^+$ T$_{SCM}$s or vehicle-treated control cells (or SP naive T cells) were mixed with the same number of newly isolated and CFSE-labeled (10 μM) SP cells and then injected intravenously into the CD45.1 recipients. The recipients were sacrificed after 24 hours, and cells from SP and BM were obtained as described to measure CMTPX$^+$/CFSE$^+$ ratios by flow cytometry. The input ratio (IR = [CMTPX]$_{input}$/[CFSE]$_{input}$) was assessed using an aliquot. HI was calculated as the ratio of [CMTPX]$_{tissue}$/[CFSE]$_{tissue}$ to [CMTPX]$_{input}$/[CFSE]$_{input}$. For instance, a HI of 1 indicates that the frequency of CMTPX-staining cells was equivalent to that of naive cells labeled with CFSE.

B16 Murine Model

B16 cells were kindly provided by Professor Jie Zhou and B16-OVA cells were established as described.[31,54] Briefly, we extracted OVA mRNA from hen oviduct and obtained cDNA by RT. OVA-expressing plasmid was constructed by inserting the OVA cDNA into retroviral vector plasmid pMSCV-puro (Clontech Laboratories Inc.) to generate plasmid pMSCV-OVA. pMSCV-OVA was cotransfected with the pIK packaging plasmid into 293T cells using the calcium phosphate transfection method. Forty-eight hours after transfection, supernatants were collected and incubated with B16 cells. The transfected cells were incubated for 24 hours in the presence of polybrene (2.5 μg/mL; Sigma-Aldrich). Puromycin (4 μg/mL; Sigma-Aldrich) was then used to select the stably transfected cells over a 12-day period. Next, C57BL/6J mice were injected intradermally with 1.5×10^6 B16-OVA cells. After 10 days, 5×10^4 OVA-specific T$_{SCM}$s, which were isolated from SP or BM of CD45.1 recipient mice after injection of OVA (0.5 mg per mouse) with CFA and TWS119 (40 mg/kg), were adoptively transferred into the tumor-bearing WT mice. The tumor burden was measured by testing tumor size and survival rates.

REFERENCES

1. Zhang Y, Joe G, Hexner E, et al. Host-reactive CD8+ memory stem cells in graft-versus-host disease. *Nat Med.* 2005;11:1299–1305.
2. Gattinoni L, Zhong XS, Palmer DC, et al. Wnt signaling arrests effector T cell differentiation and generates CD8+ memory stem cells. *Nat Med.* 2009;15:808–813.
3. Gattinoni L, Lugli E, Ji Y, et al. A human memory T cell subset with stem cell-like properties. *Nat Med.* 2011;17:1290–1297.
4. Buzon MJ, Sun H, Li C, et al. HIV-1 persistence in CD4+ T cells with stem cell-like properties. *Nat Med.* 2014;20:139–142.
5. Cartwright EK, McGary CS, Cervasi B, et al. Divergent CD4+ T memory stem cell dynamics in pathogenic and nonpathogenic simian immunodeficiency virus infections. *J Immunol.* 2014;192:4666–4673.
6. Flynn JK, Gorry PR. Stem memory T cells (TSCM)—their role in cancer and HIV immunotherapies. *Clin Transl Immunol.* 2014;3:e20.
7. Ribeiro SP, Milush JM, Cunha-Neto E, et al. The CD8+ memory stem T cell (TSCM) subset is associated with improved prognosis in chronic HIV-1 infection. *J Virol.* 2014;88:13836–13844.
8. Tabler CO, Lucera MB, Haqqani AA, et al. CD4+ memory stem cells are infected by HIV-1 in a manner regulated in part by SAMHD1 expression. *J Virol.* 2014;88:4976–4986.
9. Lugli E, Dominguez MH, Gattinoni L, et al. Superior T memory stem cell persistence supports long-lived T cell memory. *J Clin Invest.* 2013;123:594–599.
10. Mateus J, Lasso P, Pavia P, et al. Low frequency of circulating CD8+ T stem cell memory cells in chronic chagasic patients with severe forms of the disease. *PLoS Negl Trop Dis.* 2015;9:e3432.
11. Flynn JK, Paukovics G, Cashin K, et al. Quantifying susceptibility of CD4+ stem memory T-cells to infection by laboratory adapted and clinical HIV-1 strains. *Viruses.* 2014;6:709–726.
12. Cashin K, Paukovics G, Jakobsen MR, et al. Differences in coreceptor specificity contribute to alternative tropism of HIV-1 subtype C for CD4(+) T-cell subsets, including stem cell memory T-cells. *Retrovirology.* 2014;11:97.
13. Cieri N, Oliveira G, Greco R, et al. Generation of human memory stem T cells upon haploidentical T-replete hematopoietic stem cell transplantation. *Blood.* 2015;125:2865–2874.
14. Cieri N, Camisa B, Cocchiarella F, et al. IL-7 and IL-15 instruct the generation of human memory stem T cells from naive precursors. *Blood.* 2013;121:573–584.
15. Biasco L, Scala S, Basso Ricci L, et al. In vivo tracking of T cells in humans unveils decade-long survival and activity of genetically modified T memory stem cells. *Sci Transl Med.* 2015;7:273ra213.
16. Mercier FE, Ragu C, Scadden DT. The bone marrow at the crossroads of blood and immunity. *Nat Rev Immunol.* 2012;12:49–60.
17. Becker TC, Coley SM, Wherry EJ, et al. Bone marrow is a preferred site for homeostatic proliferation of memory CD8 T cells. *J Immunol.* 2005;174:1269–1273.
18. Mazo IB, Honczarenko M, Leung H, et al. Bone marrow is a major reservoir and site of recruitment for central memory CD8 + T cells. *Immunity.* 2005;22:259–270.
19. Tokoyoda K, Egawa T, Sugiyama T, et al. Cellular niches controlling B lymphocyte behavior within bone marrow during development. *Immunity.* 2004;20:707–718.
20. Tokoyoda K, Zehentmeier S, Hegazy AN, et al. Professional memory CD4+ T lymphocytes preferentially reside and rest in the bone marrow. *Immunity.* 2009;30:721–730.
21. Tokoyoda K, Hauser AE, Nakayama T, et al. Organization of immunological memory by bone marrow stroma. *Nat Rev Immunol.* 2010;10:193–200.
22. Scadden DT. The stem-cell niche as an entity of action. *Nature.* 2006;441:1075–1079.
23. Chenery AL, Antignano F, Hughes MR, et al. Chronic *Trichuris muris* infection alters hematopoiesis and causes IFN-gamma-expressing T-cell accumulation in the mouse bone marrow. *Eur J Immunol.* 2016;46:2587–2596.
24. Pinyopich A, Ditta GS, Savidge B, et al. Assessing the redundancy of MADS-box genes during carpel and ovule development. *Nature.* 2003;424:85–88.
25. Di Rosa F, Gebhardt T. Bone marrow T cells and the integrated functions of recirculating and tissue-resident memory T cells. *Front Immunol.* 2016;7:51.
26. Okhrimenko A, Grun JR, Westendorf K, et al. Human memory T cells from the bone marrow are resting and maintain long-lasting systemic memory. *Proc Natl Acad Sci USA.* 2014;111:9229–9234.
27. Kudernatsch RF, Letsch A, Guerreiro M, et al. Human bone marrow contains a subset of quiescent early memory CD8+T

cells characterized by high CD127 expression and efflux capacity. *Eur J Immunol.* 2014;44:3532–3542.

28. Cassese G, Parretta E, Pisapia L, et al. Bone marrow CD8 cells down-modulate membrane IL-7Ralpha expression and exhibit increased STAT-5 and p38 MAPK phosphorylation in the organ environment. *Blood.* 2007;110:1960–1969.

29. Quinci AC, Vitale S, Parretta E, et al. IL-15 inhibits IL-7Rα expression by memory-phenotype CD8+T cells in the bone marrow. *Eur J Immunol.* 2012;42:1129–1139.

30. Sugiyama T, Kohara H, Noda M, et al. Maintenance of the hematopoietic stem cell pool by CXCL12-CXCR4 chemokine signaling in bone marrow stromal cell niches. *Immunity.* 2006; 25:977–988.

31. Feuerer M, Beckhove P, Garbi N, et al. Bone marrow as a priming site for T-cell responses to blood-borne antigen. *Nat Med.* 2003;9:1151–1157.

32. Milo I, Sapoznikov A, Kalchenko V, et al. Dynamic imaging reveals promiscuous crosspresentation of blood-borne antigens to naive CD8+ T cells in the bone marrow. *Blood.* 2013;122:193–208.

33. Hardy RR, Carmack CE, Shinton SA, et al. Resolution and characterization of pro-B and pre-pro-B cell stages in normal mouse bone marrow. *J Exp Med.* 1991;173:1213–1225.

34. Mazo IB, von Andrian UH. Adhesion and homing of blood-borne cells in bone marrow microvessels. *J Leukoc Biol.* 1999; 66:25–32.

35. Feuerer M, Beckhove P, Bai L, et al. Therapy of human tumors in NOD/SCID mice with patient-derived reactivated memory T cells from bone marrow. *Nat Med.* 2001;7:452–458.

36. Lugli E, Gattinoni L, Roberto A, et al. Identification, isolation and in vitro expansion of human and nonhuman primate T stem cell memory cells. *Nat Protoc.* 2013;8:33–42.

37. Kunzmann V, Bauer E, Feurle J, et al. Stimulation of gammadelta T cells by aminobisphosphonates and induction of antiplasma cell activity in multiple myeloma. *Blood.* 2000;96:384–392.

38. Shibata K, Yamada H, Nakamura R, et al. Identification of CD25+ T cells as fetal thymus-derived naturally occurring IL-17 producers. *J Immunol.* 2008;181:5940–5947.

39. Hasegawa E, Sonoda KH, Shichita T, et al. IL-23-independent induction of IL-17 from gammadeltaT cells and innate lymphoid cells promotes experimental intraocular neovascularization. *J Immunol.* 2013;190:1778–1787.

40. Parretta E, Cassese G, Barba P, et al. CD8 cell division maintaining cytotoxic memory occurs predominantly in the bone marrow. *J Immunol.* 2005;174:7654–7664.

41. Kambayashi T, Assarsson E, Lukacher AE, et al. Memory CD8+ T cells provide an early source of IFN-gamma. *J Immunol.* 2003;170:2399–2408.

42. Driessens G, Zheng Y, Gajewski TF. β-catenin does not regulate memory T cell phenotype. *Nat Med.* 2010;16:513–514.

43. Gattinoni L, Ji Y, Restifo NP. Reply to: "β-catenin does not regulate memory T cell phenotype". *Nat Med.* 2010;16: 514–515.

44. Springer TA. Adhesion receptors of the immune system. *Nature.* 1990;346:425–434.

45. Koni PA, Joshi SK, Temann UA, et al. Conditional vascular cell adhesion molecule 1 deletion in mice: impaired lymphocyte migration to bone marrow. *J Exp Med.* 2001;193:741–754.

46. Ley K, Kansas GS. Selectins in T-cell recruitment to non-lymphoid tissues and sites of inflammation. *Nat Rev Immunol.* 2004;4:325–335.

47. Levesque JP, Zannettino AC, Pudney M, et al. PSGL-1-mediated adhesion of human hematopoietic progenitors to P-selectin results in suppression of hematopoiesis. *Immunity.* 1999;11:369–378.

48. Veerman KM, Carlow DA, Shanina I, et al. PSGL-1 regulates the migration and proliferation of CD8(+) T cells under homeostatic conditions. *J Immunol.* 2012;188:1638–1646.

49. Lee PP, Yee C, Savage PA, et al. Characterization of circulating T cells specific for tumor-associated antigens in melanoma patients. *Nat Med.* 1999;5:677–685.

50. Valmori D, Dutoit V, Lienard D, et al. Naturally occurring human lymphocyte antigen-A2 restricted CD8+ T-cell response to the cancer testis antigen NY-ESO-1 in melanoma patients. *Cancer Res.* 2000;60:4499–4506.

51. Guba M, von Breitenbuch P, Steinbauer M, et al. Rapamycin inhibits primary and metastatic tumor growth by antiangiogenesis: involvement of vascular endothelial growth factor. *Nat Med.* 2002;8:128–135.

52. Gondek DC, Lu LF, Quezada SA, et al. Cutting edge: contact-mediated suppression by CD4+CD25+ regulatory cells involves a granzyme B-dependent, perforin-independent mechanism. *J Immunol.* 2005;174:1783–1786.

53. Mora JR, Bono MR, Manjunath N, et al. Selective imprinting of gut-homing T cells by Peyer's patch dendritic cells. *Nature.* 2003;424:88–93.

54. Moore MW, Carbone FR, Bevan MJ. Introduction of soluble protein into the class I pathway of antigen processing and presentation. *Cell.* 1988;54:777–785.